Electronic Supplementary Material (ESI) for Journal of Materials Chemistry C.

Supporting Information

2D $ZnIn_2S_4$ nanosheets in-situ growth on sulfur-doped porous $Ti_3C_2T_x$ MXene 3D multi-functional architectures for photocatalytic H_2 evolution

Ming Du,[a] Lutao Li,[a] Shilei Ji,[a] Taomiao Wang,[a] Yile Wang,[a] Jian Zhang,*[a, b] Xing'ao Li,*[a, b]

Dr. Ming Du, Lutao Li, Dr. Shilei Ji, Taomiao Wang Dr. Yile Wang, Prof. Jian Zhang, Prof. Xing´ao Li.

[a] Key Laboratory for Organic Electronics and Information Displays & Institute of Advanced Materials (IAM), Jiangsu National Synergetic Innovation Center for Advanced Materials (SICAM), Nanjing University of Posts & Telecommunications, Nanjing 210023, PR China

Email: lxahbmy@126.com; iamjzhang@njupt.edu.cn.

[b] New Energy Technology Engineering Lab of Jiangsu Province, School of Science, Nanjing University of Posts & Telecommunications (NUPT), Nanjing 210023, PR China

Keywords: porous $Ti_3C_2T_x$, sulfur-doped, Ti-S bonds, 3D architecture, photocatalytic H_2 evolution

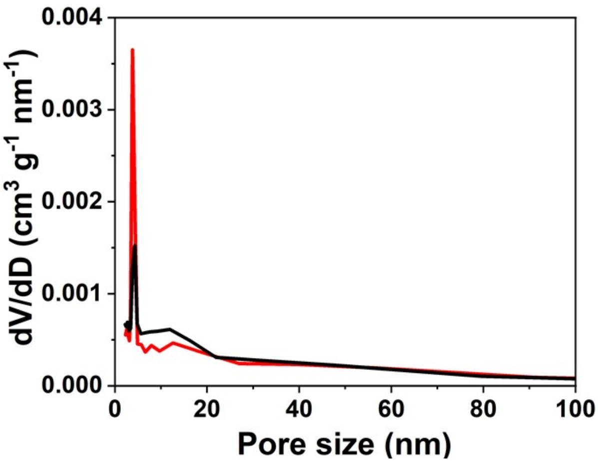

Fig. S1. The pore size distribution curves of the $ZnIn_2S_4$ and S-doped $Ti_3C_2T_x$@$ZnIn_2S_4$ composites

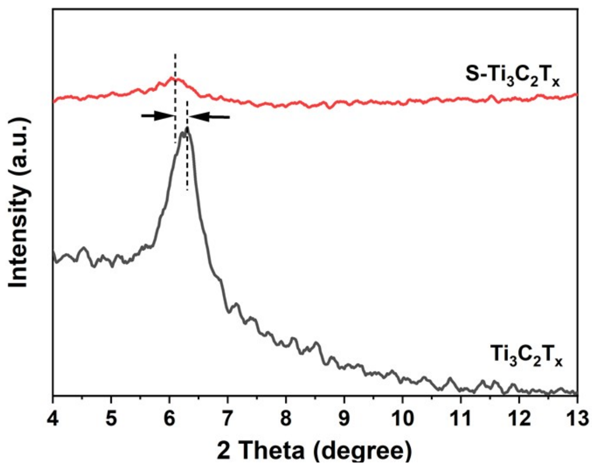

Fig. S2. X-ray diffraction patterns of $Ti_3C_2T_x$ and S-doped $Ti_3C_2T_x$.

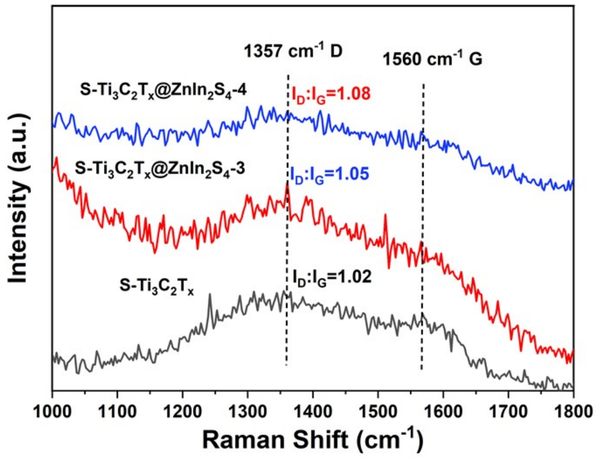

Fig. S3. Raman spectroscopy of S-doped $Ti_3C_2T_x$ and $S\text{-}Ti_3C_2T_x@ZnIn_2S_4$ composites.

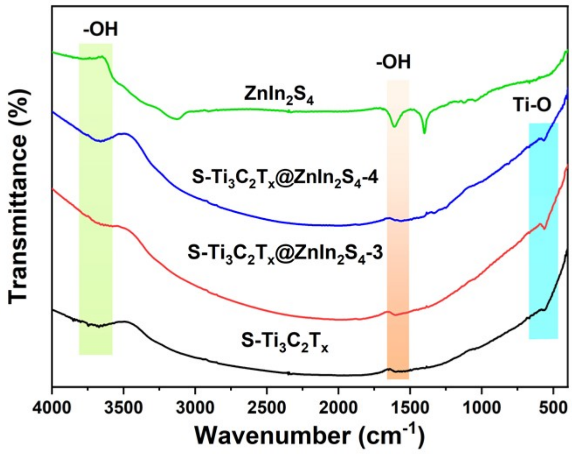

Fig. S4. FT-IR spectra of $ZnIn_2S_4$, $S\text{-}Ti_3C_2T_x@ZnIn_2S_4$ composites, and S-doped $Ti_3C_2T_x$

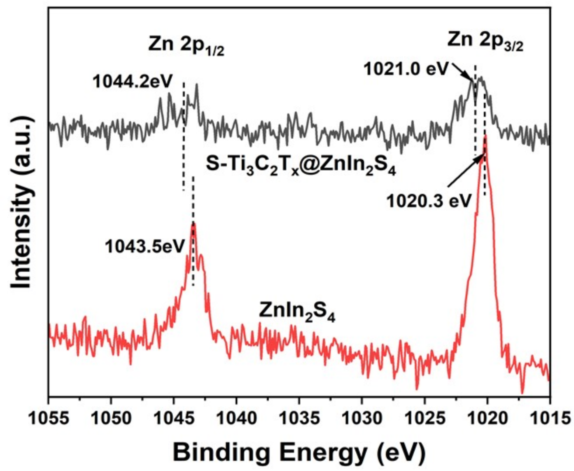

Fig. S5. Zn 2p of $ZnIn_2S_4$ and $S\text{-}Ti_3C_2T_x@ZnIn_2S_4$ composites.

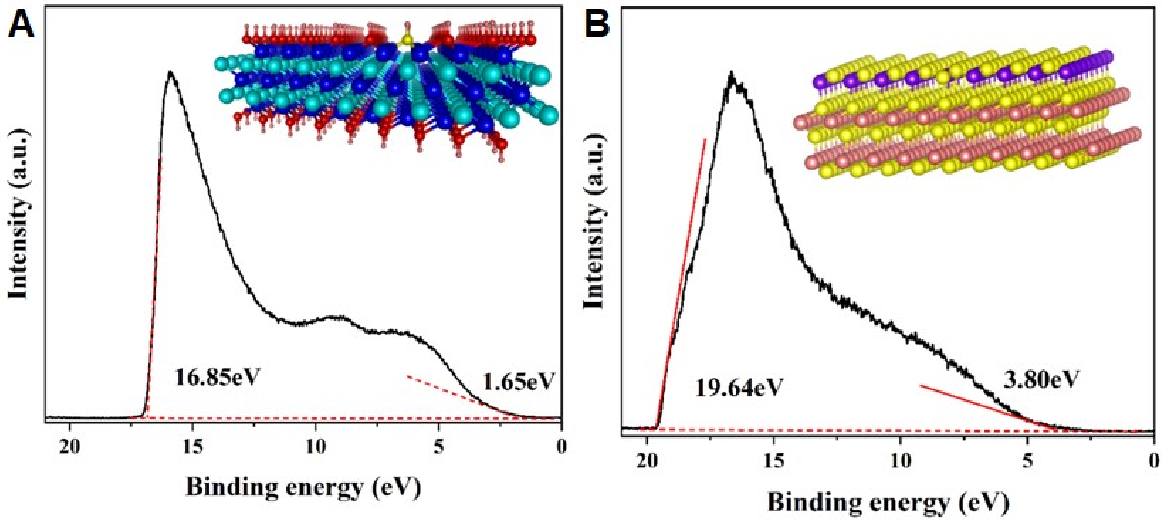

Fig. S6. UPS spectra for A) S doped $Ti_3C_2T_x$ and B) $ZnIn_2S_4$

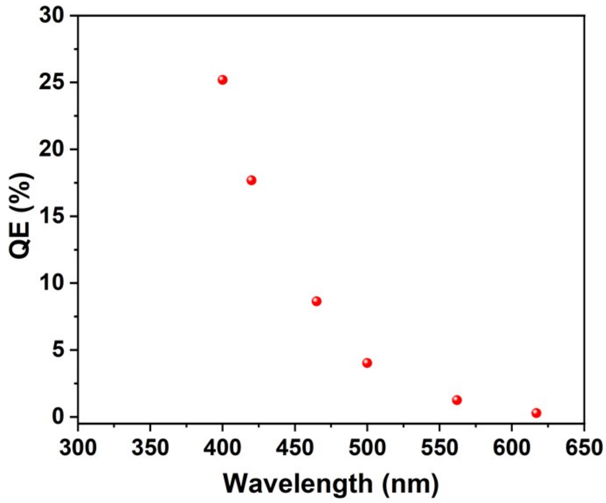

Fig. S7. The QE values of S-$Ti_3C_2T_x$@$ZnIn_2S_4$-3 at different wavelength

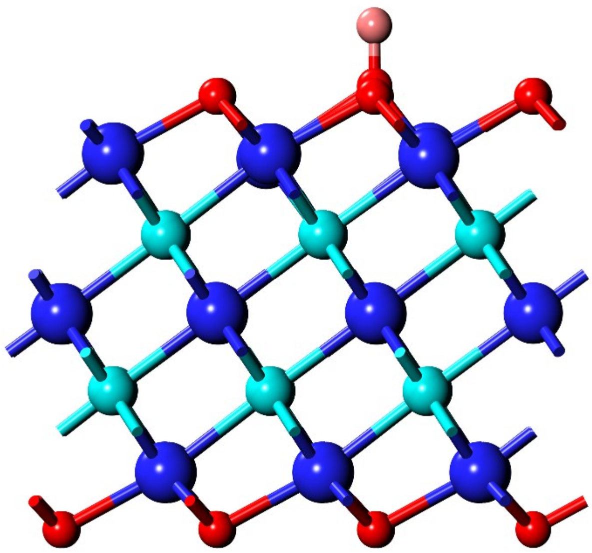

Fig. S8. Side views of the pure $Ti_3C_2T_x$.

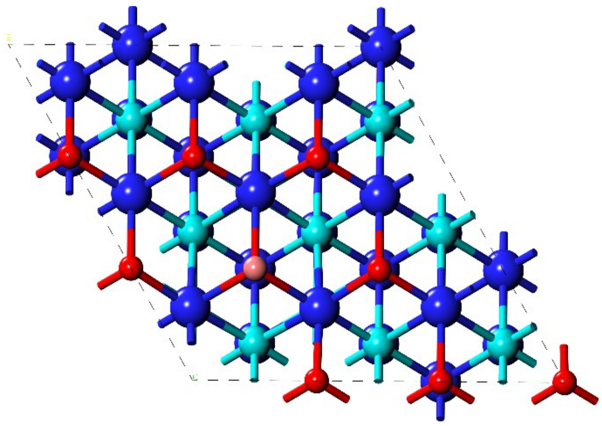

Fig. S9. Top views of the pure $Ti_3C_2T_x$.

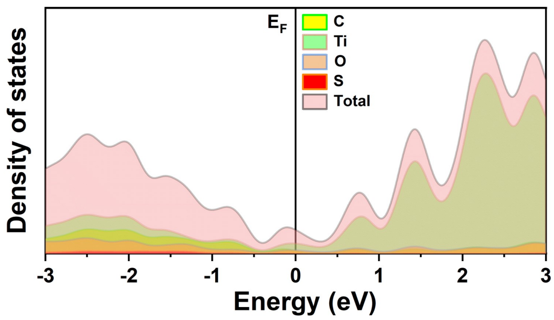

Fig. S10. Density of states of the S doped $Ti_3C_2T_x$.

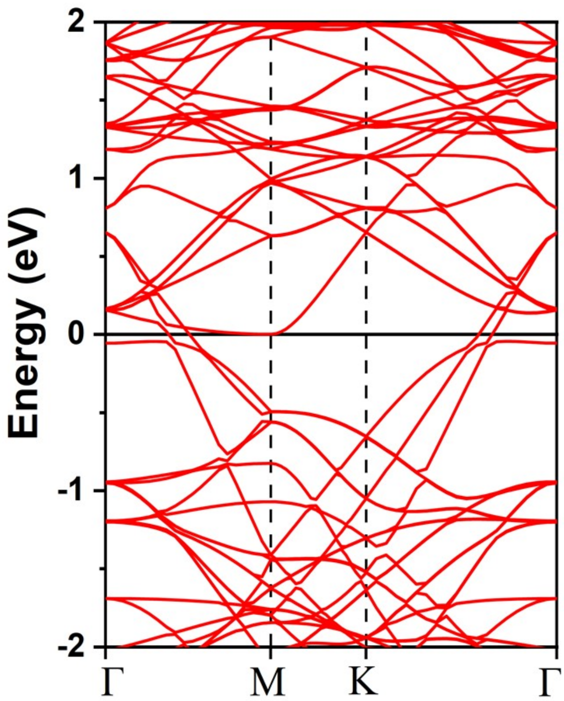

Fig. S11. The electronic band structure of the pure $Ti_3C_2T_x$.

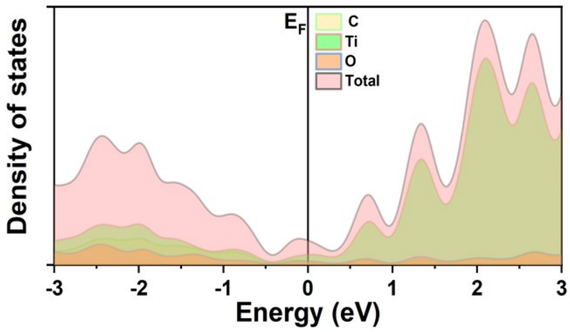

Fig. S12. The density of states of the pure $Ti_3C_2T_x$.

Table S1. Comparison of the photocatalytic H_2 evolution activity for some previous reports photocatalysts

Photocatalyst	Light source	sacrificial agent	H_2 evolution rate (mmol $h^{-1}g^{-1}$)	H_2 production QE（%）	Ref.
CdS/Ti_3C_2	300 W Xe arc lamp ($\lambda \geq 400$ nm)	TEOA	3.1765	2.28 (λ=420nm)	[1]
$CuInS_2/TiO_2$	300 W Xe lamp ($\lambda \geq 420$ nm)	MEOH	0.655	None	[2]
$CNFs/MoS_2/ZnIn_2S_4$	300 W Xe lamp ($\lambda \geq 400$ nm)	aqueous solution	0.151	20.88 (λ=365nm)	[3]
$NiCo_2S_4/ZnIn_2S_4$	300 W Xe lamp ($\lambda \geq 400$ nm)	Na_2S/Na_2SO_3	0.77	1.2 (λ=420nm)	[4]
$MXene/ZnIn_2S_4$	300 W Xe lamp ($\lambda \geq 400$ nm)	TEOA	3.475	11.14 (λ=420nm)	[5]
$BiVO_4/Ti_3C_2$	300 W Xe arc lamp ($\lambda \geq 420$ nm)	methanol solution	0.196	1.47 (λ=420nm)	[6]
ZnIn2S4/S, N co-doped carbon	300 W Xe lamp	TEOA	2.937	19.47 (λ=435nm)	[7]
$ZnIn_2S_4$-S/CNTs/RP	350 W Xe lamp	Na_2S/Na_2SO_3	1.640	None	[8]
$CuInS_2@C_3N_4$	350 W Xe lamp ($\lambda \geq 420$ nm).	Na_2S/Na_2SO_3	0.373	4.32 (λ=400nm)	[9]
TiO_2/Ti_3C_2/g-C_3N_4	300 W Xe lamp ($\lambda \geq 420$ nm).	TEOA	1.409	None	[10]
$Ti_3C_2@TiO_2/ZnIn_2S_4$	300 W Xe lamp ($\lambda \geq 400$ nm)	Na_2S/Na_2SO_3	1.186	None	[11]
$CdS/ZnIn_2S_4$	300 W Xe lamp	Na_2S/Na_2SO_3	3.072	15.9 (λ=420nm)	[12]
NH_2-MIL-125(Ti) @$ZnIn_2S_4$/CdS	300 W Xe lamp ($\lambda \geq 400$ nm)	lactic acid	2.367	None	[13]
$WO_3/ZnIn_2S_4$	300 W Xenon arc lamp ($\lambda \geq 420$ nm)	Na_2S/Na_2SO_3	1.945	18.68 (λ=420nm)	[14]

UiO-66/$ZnIn_2S_4$	300 W Xe lamp ($\lambda \geq 400$ nm)	TEOA	3.062	19.39 (λ=400nm)	[15]
S-$Ti_3C_2T_x$/$ZnIn_2S_4$	300 W Xe lamp （$\lambda \geq 400$ nm)	Na_2S/Na_2SO_3	3.058	17.68 (λ=420nm)	This work

1 B. Sun, P. Qiu, Z. Liang, Y. Xue, X. Zhang, L. Yang, H. Cui and J. Tian, *Chem. Eng. J.*, 2021, **406**, 127177.

2 H. Hou, Y. Yuan, S. Cao, Y. Yang, X. Ye and W. Yang, *J. Mater. Chem. C*, 2020, **8**, 11001-11007.

3 Y. Sun, C. Xue, L. Chen, Y. Li, S. Guo, Y. Shen, F. Dong, G. Shao and P. Zhang, *Sol. RRL*, 2021, **5**, 2000722.

4 K. Wu, R. Jiang, Y. Zhao, L. Mao, X. Gu, X. Cai and M. Zhu, *J. Colloid Interface Sci.*, 2022, **619**, 339-347.

5 G. Zuo, Y. Wang, W. L. Teo, A. Xie, Y. Guo, Y. Dai, W. Zhou, D. Jana, Q. Xian and W. Dong, *Angewandte Chemie*, 2020, **132**, 11383-11388.

6 Y. Li, Y. Liu, D. Xing, J. Wang, L. Zheng, Z. Wang, P. Wang, Z. Zheng, H. Cheng and Y. Dai, *Appl. Catal., B*, 2021, **285**, 119855.

7 X. Fu, C. Huang, J. Wen, Y. Du and X. Zheng, *Int. J. Hydrogen Energy*, 2021, **46**, 17697-17707.

8 L. Liu, J. Liu, W. Yang, J. Wan, F. Fu and D. Wang, *J. Colloid Interface Sci.*, 2022, **608**, 482-492.

9 J. Luo, Z. Lin, Y. Zhao, S. Jiang and S. Song, *Chin. J. Catal.*, 2020, **41**, 122-130.

10 V. Q. Hieu, T. C. Lam, A. Khan, T.-T. T. Vo, T.-Q. Nguyen, V. D. Doan and V. A. Tran, *Chemosphere*, 2021, **285**, 131429.

11 K. Huang, C. Li and X. Meng, *J. Colloid Interface Sci.*, 2020, **580**, 669-680.

12 Y. Zhu, J. Chen, L. Shao, X. Xia, Y. Liu and L. Wang, *Appl. Catal., B*, 2020, **268**, 118744.

13 S. Zhang, M. Du, Z. Xing, Z. Li, K. Pan and W. Zhou, *Appl. Catal., B*, 2020, **262**, 118202.

14 Y. Wang, D. Chen, Y. Hu, L. Qin, J. Liang, X. Sun and Y. Huang, *Sustainable Energy Fuels*, 2020, **4**, 1681-1692.

15 X. Peng, L. Ye, Y. Ding, L. Yi, C. Zhang and Z. Wen, *Appl. Catal., B*, 2020, **260**, 118152.